

# Topological invariants can be used to quantify complexity in abstract paintings



Elsa M. de la Calleja, Roberto Zenit\*

Instituto de Investigaciones en Materiales, Universidad Nacional Autónoma de México, Apdo. Postal 70–360, Ciudad Universitaria, D.F. 04510, México

## ARTICLE INFO

### Article history:

Received 19 January 2017

Revised 7 March 2017

Accepted 30 March 2017

Available online 12 April 2017

### Keywords:

Complexity

Topological invariants

Abstract art

Art assessment

## ABSTRACT

Abstract art screams of complexity: its visual language purposely creates complex images that are a distorted artist-driven vision of the real world. Complexity can be recognized from either the composition, form, color, brightness, among other aspects. In this paper we show that it is possible to objectively assess the complexity of abstract paintings by determining the values of the Betti numbers associated with the image. These quantities, which are topological invariants, capture the amount of connectivity and spatial distribution of the paint traces. We apply this analysis to a series of abstract paintings, demonstrating that the complexity of Jackson Pollock paintings produced by his famous dripping technique, is superior compared with many other abstract paintings by different authors. Opposed to what was previously discussed considering only fractal properties, the complexity does not simply increase with time; instead, it displays a local maximum at a certain year which coincides with the time when Pollock perfected his technique. This tool has been used before to measure complexity in other scientific areas, but not for art assessment.

© 2017 Elsevier B.V. All rights reserved.

## 1. Introduction

Can abstract art be quantified? Some studies have argued that different features of artistic images can be characterized mathematically, taking into account specific features such as color, brightness, distribution of shapes or contours [1–4]. However, the majority of judgments, trying to qualify the aesthetic perception depend on environment, culture, age, color preferences or the personality of the judge [5,6]. Among the ways that can be used to describe, and also quantify art, a notable idea is its complexity. There are some examples of the use complexity to describe art [4,7–10]. However, when trying to make this description quantifiable, the measurement always relays on the aesthetic perception [6] which is not quantifiable.

Since complexity is a signature of the behavior of many physical phenomena, understood as the dynamics of the interaction of diverse and numerous elements that produce emergent behavior [11], tools are needed to extract relevant course information from observations. One way to accomplish this, for the case of images, is the determination of self-similarity properties. This idea has already been used for the case of artistic painting [12–15]. Some of

these studies have been very well received by the art community [16,17]; however, some authors have questioned the extent of their applicability [18,19].

We propose the use of a new technique to quantify complexity in abstract paintings using a well-established mathematical tool: algebraic topology. This branch of mathematics deals with the description of form and shape of functions and spaces [20]. The Betti numbers are quantities that can be used to distinguish  $n$ -dimensional topological spaces; they essentially measure the connectivity of such spaces and has been used to measure complexity in other scientific areas [21–25]. Note that the Physics Nobel prize of 2016 was awarded, in part, for the use of topological invariants to characterize the structure of materials [26]. Since these topological invariants extract the geometrical essence of an image, we argue that they can be used as a fundamental and objective measure of complexity of abstract art.

In order to test this idea, we selected works by the American abstract expressionist Jackson Pollock to measure their complexity. We chose this particular artist because there have been quantifications of the complexity of his paintings [12–15,25,27–30]. These studies give a measure of complexity but its meaning and implications remain controversial. To take our proposed technique further, we also select paintings from other abstract artists which, to the naked eye, resemble the composition style or technique used by Jackson Pollock to make direct comparisons.

\* Corresponding author.

E-mail address: [zenit@unam.mx](mailto:zenit@unam.mx) (R. Zenit).

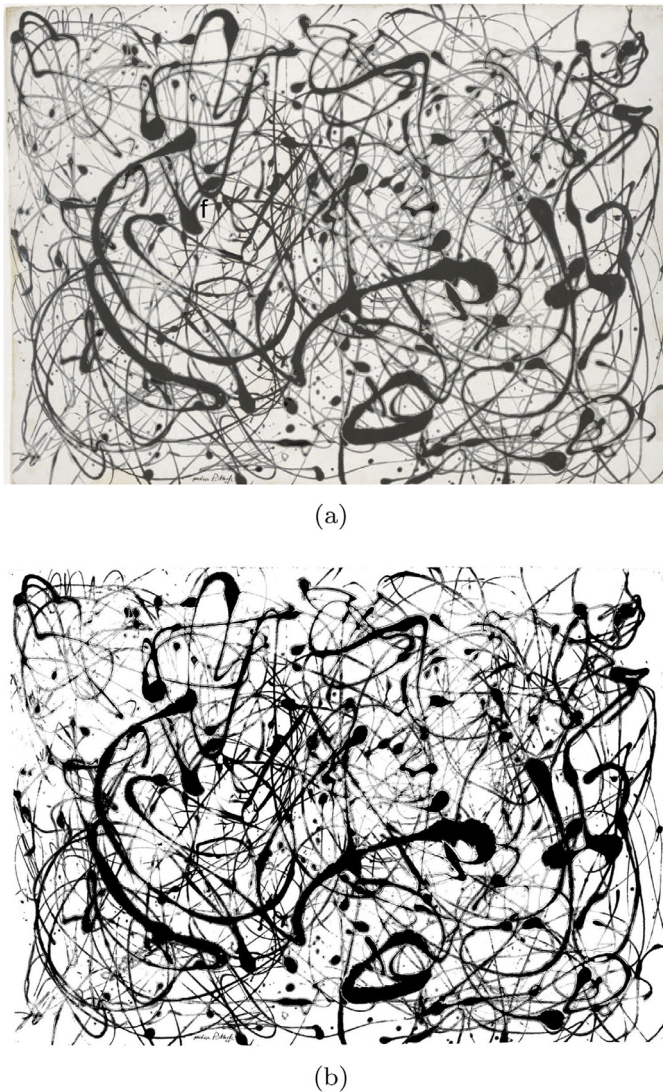


**Fig. 1.** A typical Jackson Pollock painting used to quantify complexity using Betti numbers. (a) Number 14: Gray, Jackson Pollock, 1948, original image; (b) binarized image. Reproduced with permission from the Yale University Art Gallery.

## 2. Methodology

### 2.1. Image processing

The images were processed using the ImageJ software [31]. In a short, high resolution images were transformed, through standard image processing algorithms, into binary images. Such binary images are amenable for the calculation of the Betti numbers using the software CHOMP [32]. The images were also size-filtered. Groups of pixels smaller than five pixels were discarded. High resolution images were obtained from different sources (See Tables 1 and 2). Each image was transformed into an 8-bit grey resolution and then the brightness was adjusted to obtain the highest number of dark strokes. The image was then binarized taking into consideration a threshold level of 132 a.u. Fig. 1 shows this process. The binary image is taken to represent a 2-dimensional topological space for which two Betti numbers,  $\beta_0$  and  $\beta_1$ , can be calculated.

### 2.2. Selection of abstract paintings

Images with only a few colored well-defined dark strokes (or lines) over a light background were chosen. We selected the works

of Jackson Pollock from the dripping period that fulfilled this requirement, which include paintings made from 1946 until 1951. Works from other abstract expressionist artists were chosen following the same guidelines. The list of all works is included in Tables 1 and 2.

### 2.3. Calculation of topological invariants

Once the images were binarized, the software CHOMP was used [32]. In short, the algorithm of this software calculates the local elementary reductions and collapses to compute the homology of the images. More details on the algorithm can be found in [33]. Note that the algorithm does not count the holes that appear on the image edges (incomplete or cut holes are not counted).

Fig. 2(a) shows a zoom of the binary image shown in Fig. 1(b) for which these quantities were measured. For the image shown  $\beta_0 = 3$ . Broadly speaking  $\beta_0$  measures the number of connected regions in a region. Single drops that do not touch other traces are counted as separated regions. As more traces or drops are deposited on the canvas without overlapping one another,  $\beta_0$  increases.

On the other hand, the second Betti number,  $\beta_1$ , measures the number of holes in a region. Fig. 2(c) shows the number of holes in the images represented by  $\beta_1 = 19$ . Even if numerous traces are placed on the canvas to form one object, the spaces left in between them would be counted as holes; therefore, it quantifies how filled of traces the object is. If the traces are connected and surround an empty area, the  $\beta_1$  also increase. To illustrate the change of the Betti numbers with the visual properties of an image, and its complexity, we applied the technique to series of synthetically produced abstract images, described below.

### 2.4. Synthetic abstract paintings

To illustrate the meaning of the topological invariants, synthetic abstract images were created with a Matlab© script. We placed  $N$  straight black lines over a white two-dimensional space with a fixed area of  $1 \times 1$  (arbitrary units). Each line had fixed length,  $L$ , and width,  $W$ . The position and angle of each line is randomly selected such that the line does not lay beyond the width and height of the work space. Typical images are shown in Fig. 3. Three examples are shown: the length of the lines increases from case (a) to (c), but to preserve the surface area of each line the thickness is reduced. Therefore (a) shows images for short-thick lines, while (c) shows lines which are long and thin.

Fig. 4 shows the values of  $\beta_0$  and  $\beta_1$  for the synthetic abstract images as a function of the number of lines,  $N$ . The three cases shown correspond to those depicted in Fig. 3: short thick lines (L1W4, blue markers,  $L = 0.1$ ,  $W = 4$ ); lines of medium length and thickness (L2W2, red markers,  $L = 0.2$ ,  $W = 2$ ); and long thin lines (L4W1, black markers,  $L = 0.4$ ,  $W = 1$ ). To test the repeatability of the measurements, the case of  $N = 200$  for the L2W2 lines was repeated 10 times. The error bars on  $\beta_0$  and  $\beta_1$  for that condition denote the variability of the results.

For all cases  $\beta_0$  increases linearly with  $N$  and  $\beta_1 = 0$ , for small number of lines. This is expected for non-touching lines since  $\beta_0$  measures the number of connected regions and  $\beta_1$  measures the number of holes. As  $N$  increases and reaches a sufficiently large value, the lines inevitably begin to cross; therefore,  $\beta_0$  ceases to increase while  $\beta_1$  begins to increase in proportion with  $N^2$ . This quadratic dependence denotes an increase the number of holes which is proportional to the areas created by the new crossings. As  $N$  increases further, more lines are placed over each other; therefore the number of independently connected objects begins to decrease yet the number of holes continues to increase. Beyond a

**Table 1**  
Selected paintings by Jackson Pollock, in which the dripping technique was mostly used.

Number	Name	Year	Size (cm <sup>2</sup> )	Main colors	Location and Source
P1	One: Number 31	1950	269.5 × 530.8	Black, White, Navajo, White4, SteelBlue4	The Museum of Modern Art. <a href="http://www.moma.org/collection/works/78386">www.moma.org/collection/works/78386</a>
P2	Autumn Rhythm	1950	266.7 × 525.8	Black NavajoWhite4, White	Metropolitan Museum of Art. <a href="http://www.metmuseum.org/art/collection/search/488978">www.metmuseum.org/art/collection/search/488978</a>
P3	Number 28	1950	173 × 266.7	Black, Seashell2, Wheat4	Metropolitan Museum of Art. <a href="http://www.metmuseum.org/art/collection/search/490217">www.metmuseum.org/art/collection/search/490217</a>
P4	Echo: Number 25	1951	233.4 × 218.4	Black	Museum of Modern Art. <a href="http://www.moma.org/collection/works/79251?locale=en">www.moma.org/collection/works/79251?locale=en</a>
P5	Number 10	1949	46.04 × 272.4	Black, Wheat3, Snow1, SteelBlue4	Museum of Fine Arts Boston. <a href="http://www.mfa.org/collections/object/number-10-1949-34114">www.mfa.org/collections/object/number-10-1949-34114</a>
P6	Number 29	1950	121.9 × 182.9	Black, Snow4	National Gallery of Canada. <a href="http://www.wikiart.org/en/jackson-pollock/number-29-1950">www.wikiart.org/en/jackson-pollock/number-29-1950</a>
P7	Enchanted Forest	1947	221.3 × 114.6	Black, Light Apricot	The Solomon R. Guggenheim Foundation <a href="http://www.guggenheim.org/artwork/3483">www.guggenheim.org/artwork/3483</a>
P8	Number 13A	1948	94 × 297.2	White, Snow4,Black	Yale University Art Gallery. <a href="http://artgallery.yale.edu/collections/objects/60600">artgallery.yale.edu/collections/objects/60600</a>
P9	Number 32	1950	269 × 457.5	Black	Kunstsammlung Nordrhein-Westfalen. <a href="http://www.wikiart.org/en/jackson-pollock/number-32-1950">www.wikiart.org/en/jackson-pollock/number-32-1950</a>
P10	Number 15	1948	56.52 × 77.47	White, Snow3, Black	Virginia Museum of Fine Arts. <a href="http://vmfa.museum/collections/art/number-15-1948/">vmfa.museum/collections/art/number-15-1948/</a>
P11	Free Form	1946	48.9 × 35.5	Black, White, OrangeRed2	The Museum of Modern Art. <a href="http://www.moma.org/collection/works/80170?locale=en">www.moma.org/collection/works/80170?locale=en</a>
P12	Untitled: JP	1951	62.9 × 100.3	Black	Robert and Jane Meyerhoff Collection. <a href="http://elopedelart.canablog.com/archives/2009/10/02/15285905.html">elopedelart.canablog.com/archives/2009/10/02/15285905.html</a>
P13	Untitled	1951	63.5 × 98.4	Black, Orange4	Museum of Modern Art. <a href="http://www.moma.org/collection/works/37765?locale=en">www.moma.org/collection/works/37765?locale=en</a>
P14	Mural on Indian Red Ground	1950	183 × 244	Wheat1, Black, Seashell1, Snow2	Tehran Museum of Contemporary Art. <a href="http://www.wikiart.org/en/jackson-pollock/mural-on-indian-red-ground-1950">www.wikiart.org/en/jackson-pollock/mural-on-indian-red-ground-1950</a>
P15	Composition	1948	81.3 × 101.6	Snow1, SlateGray4, SteelBlue4, White, Black	New Orleans Museum of Art. <a href="http://www.jackson-pollock.org/composition.jsp">www.jackson-pollock.org/composition.jsp</a>
P16	Number 26A	1948	205 × 121.7	Black	Musee National d'Art Modern. <a href="http://www.centrepompidou.fr/cpv/resource/ckz9o9/r6krA8">www.centrepompidou.fr/cpv/resource/ckz9o9/r6krA8</a>
P17	Number 1 (Lavender Mist)	1950	221 × 299.7	Black, RosyBrown3, Snow1, Gray0, PeachPuff2	National Gallery of Art. <a href="http://www.nga.gov/collection/gallery/20centpa/20centpa-55819.html">www.nga.gov/collection/gallery/20centpa/20centpa-55819.html</a>
P18	Number 8	1949	86.6 × 180.9	Black, Wheat1, PeachPuff1, OrangeRed3, Yellow4	Neuberger Museum <a href="http://www.wikiart.org/en/jackson-pollock/number-8-detail">www.wikiart.org/en/jackson-pollock/number-8-detail</a>
P19	Cathedral	1947	181.6 × 89.1	Black, White, Snow4, Tan2	Dallas Museum of Fine Arts <a href="http://www.wikiart.org/en/jackson-pollock/cathedral-1947">www.wikiart.org/en/jackson-pollock/cathedral-1947</a>
P20	Number 1A	1948	172.7 × 264.2	Black, Whent1, Snow1, SteelBlue4, Gray0	Museum of Modern Art New York. <a href="http://www.moma.org/collection/works/78699?locale=en">www.moma.org/collection/works/78699?locale=en</a>
P21	Reflection of the big dipper	1947	111 × 91.5	Black, Royal Blue4, Snow1	Stedelijk Museum Amsterdam. <a href="http://www.jackson-pollock.org/reflection-of-the-big-dipper.jsp">www.jackson-pollock.org/reflection-of-the-big-dipper.jsp</a>
P22	Untitled	1950	44.5 × 56.6	Black	Modern Museum of Art. <a href="http://www.moma.org/collection/works/37760?locale=en">www.moma.org/collection/works/37760?locale=en</a>
P23	Number 15. Masonite	1950	55.88 × 55.88	Black, White, MistyRose2	LACMA. <a href="http://collections.lacma.org/node/229998">collections.lacma.org/node/229998</a>
P24	Lucifer	1947	267.9 × 104.1	Black, Snow1, Snow2, Snow3, OliveDrab4	Standford University Museum Art Gallery. <a href="http://www.jackson-pollock.org/index.jsp">www.jackson-pollock.org/index.jsp</a>
P25	Number 17	1949	56.5 × 72	SpringGreen4, Black, Gray0, Snow3	Contemporary Art at Sotheby's. <a href="http://wikiart.org/en/jackson-pollock/number-17-1949">wikiart.org/en/jackson-pollock/number-17-1949</a>
P26	Number 14: Gray	1948	57 × 78.5	Black, Gray0	Yale University Art Gallery. <a href="http://artgallery.yale.edu/collections/objects/33977">artgallery.yale.edu/collections/objects/33977</a>
P27	Number 4 (Gray and Red)	1948	58 × 79	Gray0, Red4, Black	Frederick R. Weisman Art Museum. <a href="http://www.wikiart.org/en/jackson-pollock/number-4-gray-and-red-1948">www.wikiart.org/en/jackson-pollock/number-4-gray-and-red-1948</a>
P28	Number 23	1948	57.5 × 78.4	Grey0, Snow1, Black	Tate Gallery. <a href="http://www.tate.org.uk/art/artworks/pollock-number-23-t00384">www.tate.org.uk/art/artworks/pollock-number-23-t00384</a>
P29	Number 18	1950	56 × 56.7	Black, Peach Puff1, Gray	Solomon R. Guggenheim Museum. <a href="http://www.guggenheim.org/artwork/3484">www.guggenheim.org/artwork/3484</a>

certain value of  $N$ , the entire space is filled with lines and both  $\beta_0$  and  $\beta_1$  decrease.

From the dependance of  $\beta_0$  and  $\beta_1$  we directly assess the topological changes of the images. Clearly, for either small or large  $N$  the image is simple; either isolated traces or one large solid blob. Therefore, an intermediate value of  $N$  will produce many connections and many holes. We therefore conjecture that the maximum complexity of an image can be found with the values of  $\beta_0$  and  $\beta_1$  are approximately the same: there is a certain balance between individually placed lines and the crosses that produce holes, among them. From the results shown in Fig. 4 we observe that the value

of  $N$  for which  $\beta_0 \approx \beta_1$  depends on the length of the lines. As the length of lines increases, the balance between Betti numbers is found for larger  $N$  values.

### 3. Results

We now apply the procedure described above to the case of actual abstract paintings. In Fig. 5 we show the measurements of Betti numbers for the artworks of Jackson Pollock enlisted in Table 1, as a function of the date of creation. Since the precise date is not known, works painted on the same year are presented as a

**Table 2**  
Paintings by other abstract expressionist who used a technique similar to Pollock's dripping.

Number	Artist	Name	Year	Size (cm)	Main colors	Source
A1	Lee Krasner	Obsidian	1962	56.1 × 76	Black	<a href="http://www.moma.org/collection/works/71667?locale=es">www.moma.org/collection/works/71667?locale=es</a>
A2	Giulio Turcato	Arcipelago	1972	80 × 100	OrangeRed2, Red3	<a href="http://www.wikiart.org/en/giulio-turcato">www.wikiart.org/en/giulio-turcato</a>
A3	C. Marcel Barbeau	Natashkouan	1956	182.9 × 213.4	Black, Green, Red	<a href="http://www.wikiart.org/en/Search/natashkouan">www.wikiart.org/en/Search/natashkouan</a>
A4	Giulio Turcato	Composizione	1971	43 × 73	RoyalBlue4, OrangeRed1	<a href="http://www.wikiart.org/en/giulio-turcato/composizione-1971">www.wikiart.org/en/giulio-turcato/composizione-1971</a>
A5	Giulio Turcato	Itinerario	1977	50 × 70	OrangeRed2, PaleTurquoise2	<a href="http://www.wikiart.org/en/giulio-turcato">www.wikiart.org/en/giulio-turcato</a>
A6	Lee Krasner	Night Creatures	1965	76.2 × 108	Black, White	<a href="http://www.metmuseum.org/art/collection/search/486683">www.metmuseum.org/art/collection/search/486683</a>
A7	Lee Krasner	Gold Stone	1969	58 × 76	Orange1, Tan1	<a href="http://www.wikiart.org/en/lee-krasner/gold-stone-1969">www.wikiart.org/en/lee-krasner/gold-stone-1969</a>
A8	Brice Marden	Letter with Red	2009	57.2 × 76.2	Black, Red3, Snow1	<a href="http://www.artnet.com/artists/brice-marden/letter-with-red-a-bC43vFuA86y8rxqHavtNDQ2">www.artnet.com/artists/brice-marden/letter-with-red-a-bC43vFuA86y8rxqHavtNDQ2</a>
A9	Brice Marden	Long Letter 1	2009	57.2 × 76.2	Black, Snow1	<a href="http://www.wikiart.org/en/brice-marden/long-letter-1-2009">www.wikiart.org/en/brice-marden/long-letter-1-2009</a>
A10	Brice Marden	Dragons	2004	102.9 × 75.7	Red3, White, Yellow3, Black	<a href="http://www.artnet.com/artists/brice-marden/dragons-a-g0iWskoFwrnSArJBYtrN5A2">www.artnet.com/artists/brice-marden/dragons-a-g0iWskoFwrnSArJBYtrN5A2</a>
A11	Jean Paul Riopelle	Jute IV	1967	104.8 × 80	Snow4, SlateBlue3	<a href="http://www.wikiart.org/en/jean-paul-riopelle/jute-iv-1967">www.wikiart.org/en/jean-paul-riopelle/jute-iv-1967</a>
A12	C. Marcel Barbeau	Froce-clat, or Brise D'Automne	1975	81.3 × 101	Black, Blue, Red	<a href="http://www.wikiart.org/en/marcel-barbeau/brise-d-automne-1975">www.wikiart.org/en/marcel-barbeau/brise-d-automne-1975</a>
A13	Lee Krasner	Untitled	1959	68.5 × 56.5	Fandango, Burdeos	<a href="http://www.wikiart.org/en/lee-krasner/untitled-1949">www.wikiart.org/en/lee-krasner/untitled-1949</a>
A14	Brion Gysin	Untitled	1959	65 × 50	Black, Yellow, Orange	<a href="http://www.artnet.com/artists/brion-gysin/untitled-a-f6lAml-M4lJYAzCj0_hUjQ2">www.artnet.com/artists/brion-gysin/untitled-a-f6lAml-M4lJYAzCj0_hUjQ2</a>
A15	Lee Krasner	Untitled	1964	56.5 × 77.2	Black, Pink, Salmao	<a href="http://www.moma.org/collection/works/33262?locale=en">www.moma.org/collection/works/33262?locale=en</a>
A16	Lee Krasner	Summer Play	1962	76.2 × 56.83	Red, Orange, Pink	<a href="http://www.wikiart.org/en/lee-krasner/summer-play-1962">www.wikiart.org/en/lee-krasner/summer-play-1962</a>
A17	Giulio Turcato	Itinerari, ca	1970–1979	50 × 70	Granate, Orange, Blue	<a href="http://www.arsvalue.ilsole24ore.com/aste/dettaglio-opera.aspx?opr=2707716&amp;ast=291&amp;ses=515">www.arsvalue.ilsole24ore.com/aste/dettaglio-opera.aspx?opr=2707716&amp;ast=291&amp;ses=515</a>
A18	Perle Fine	Untitled	1957	21.6 × 27.9	Black, Ante	<a href="http://www.wikiart.org/es/paintings-by-style/abstract-expressionism/11">www.wikiart.org/es/paintings-by-style/abstract-expressionism/11</a>
A19	Philip Guston	Untitled	1951	43.3 × 59	Black	<a href="http://www.moma.org/collection/works/37156?locale=en">www.moma.org/collection/works/37156?locale=en</a>
A20	Brice Marden	Nevis Letter no.5: to Shitao	2007–2009	57 × 76	Black	<a href="http://www.matthewmarks.com/new-york/exhibitions/2010-10-29_brice-marden/works-in-exhibition/">www.matthewmarks.com/new-york/exhibitions/2010-10-29_brice-marden/works-in-exhibition/</a>
A21	Brice Marden	Hydra Summer	1990	35.5 × 21.5	Black	<a href="http://www.matthewmarks.com/new-york/exhibitions/1991-05-07_brice-marden/works-in-exhibition/#/images/14/">www.matthewmarks.com/new-york/exhibitions/1991-05-07_brice-marden/works-in-exhibition/#/images/14/</a>
A22	Sam Francis	Beaudelaire	1986	106.7 × 149.9	Yellow3	<a href="http://www.artnet.com/artists/sam-francis/ baudelaire-jgklgllocJzKZ5nTjqMJ2">www.artnet.com/artists/sam-francis/ baudelaire-jgklgllocJzKZ5nTjqMJ2</a>
A23	Willem de Kooning	Untitled	1949–1950	48 × 64.9	Black	<a href="http://www.wikiart.org/en/willem-de-kooning/untitled-1950">www.wikiart.org/en/willem-de-kooning/untitled-1950</a>
A24	Mark Tobey	Morning Grass	1975	35.6 × 27.7	RoyalBlue2	<a href="http://www.wikiart.org/en/mark-tobey/morning-grass">www.wikiart.org/en/mark-tobey/morning-grass</a>
A25	Atsuko Tanaka	Untitled	1984	27.43 × 36.3	Black	<a href="http://www.wikiart.org/en/atsuko-tanaka/untitled-1984">www.wikiart.org/en/atsuko-tanaka/untitled-1984</a>
A26	C. Marcel Barbeau	At the chateau D'Argol	1946	55.3 × 49	Black	<a href="http://www.wikiart.org/en/marcel-barbeau/at-the-chateau-d-argol">www.wikiart.org/en/marcel-barbeau/at-the-chateau-d-argol</a>
A27	C. Marcel Barbeau	Rosier Feuilles	1946	49 × 75.5	NavajoWhite2, Wheat2, PeachPuff2	<a href="http://www.wikiart.org/en/marcel-barbeau/rosier-feuilles-1946">www.wikiart.org/en/marcel-barbeau/rosier-feuilles-1946</a>
A28	Arthur Pinajian	Landscape no. 4398	1962	40.6 × 31.8	Black	<a href="http://www.wikiart.org/en/arthur-pinajian/untitled-landscape-woodstock-no-4398-1962">www.wikiart.org/en/arthur-pinajian/untitled-landscape-woodstock-no-4398-1962</a>
A29	Brice Marden	Don't bungle the jungle	1989	26 × 51.5	Black	<a href="http://www.wikiart.org/en/Search/bungle%20the%20jungle">www.wikiart.org/en/Search/bungle%20the%20jungle</a>

single data point, which represents the mean of all of the paintings for that given year. Note that both  $\beta_0$  and  $\beta_1$  are normalized with the area of each painting,  $A$ , to allow comparison between works of different sizes. The variability of the measure is depicted by the error bars, which show the standard variation of the data set. We found that Pollock's artworks have distinctive features which are very different from those obtained for the synthetic images.

First, and in contrast with other measures of complexity [6,10,13,14], the values of  $\beta_0/A$  and  $\beta_1/A$  do not simply increase with time. The  $\beta_0/A$  number appears to remain relatively constant over time, showing a weak maximum for the year 1948. Conversely the  $\beta_1/A$  number decays in time, showing a minimum value around 1948 also. The measurements for the year 1951 do not follow this general trend. Clearly, the evolution of  $\beta_0/A$  and  $\beta_1/A$  is different than that obtained by simply adding lines randomly, as shown with the synthetic images. Upon closer inspection, the fractal dimension of Pollock's paintings reported by [29] do show a relatively constant value, for the particular range of dates considered in our study, which is consistent with the behavior of  $\beta_0/A$  reported here. This suggests that the two metrics

could be related; however, a more in depth analysis would have to be conducted to draw definite conclusions.

We surmise that the evolution of the Betti numbers can be interpreted as the evolution of the dripping technique. For early times, as the technique was not yet fully developed, more isolated traces were painted, leading to small values of  $\beta_0$  and large values of  $\beta_1$ . For the year 1948, arguably a pivotal year in the productive life of the artist, at least for this particular technique and for the selected paintings, a similar value for the number of connected regions and holes is obtained ( $\beta_0 \approx \beta_1$ ). This can be interpreted as a balance: the paintings were not oversaturated with traces yet less spaces were left without paint. A similar conclusion was found from the analysis of synthetic images. For later years, the artist continued to paint but using more traces and spilling more paint on the canvases, leading to a decrease in  $\beta_0$  and an increase in  $\beta_1$ . It is also interesting to note that both Betti numbers show significantly large variations for the year 1950 which coincides with the most volatile period in the life of Pollock [34]. Therefore, we can argue that the measurements of complexity proposed here give some indirect indication of the work of this particular artist. For

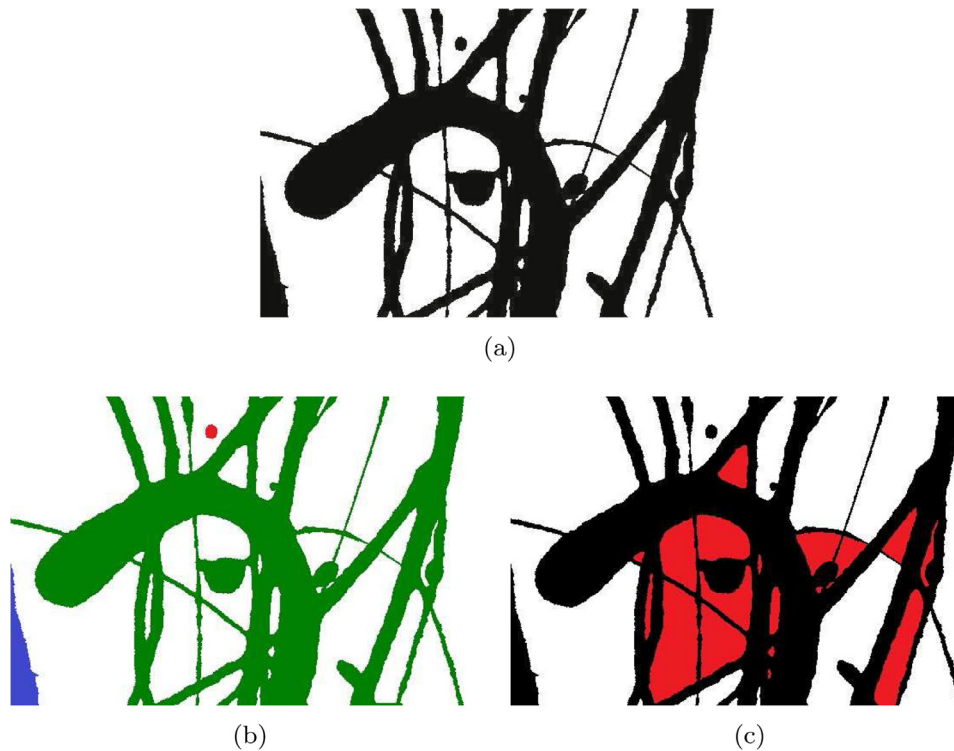


**Fig. 2.** Illustration of the meaning of the Betti numbers in an abstract painting. (a) Zoom from the binarized version of Number 14: Gray obtained from Fig. 1(b), for which  $\beta_0 = 3$  and  $\beta_1 = 19$ ; (b) shows the three regions corresponding to  $\beta_0 = 3$ , in three different colors (blue, green and red); (c) shows the 19 holes corresponding to  $\beta_1 = 19$ , all colored in red. (For interpretation of the references to color in this figure legend, the reader is referred to the web version of this article.)

1951, the measurements of  $\beta_0$  and  $\beta_1$  decrease and have approximately the same value; coincidentally, for this year, Pollock was more stable and painted in a more balanced way again. The variations of our measurements seem to agree with the different productive life periods of the painter.

#### 4. Discussion and conclusions

It is clear that the calculation of the Betti numbers allow us to quantify certain aspects of the abstract paintings by Jackson Pollock, arguably related to the complexity of the images. To end and enrich our discussion, we now offer a direct comparison of the works of Pollock with those from other abstract artists. We strived to make the comparison as a fair as possible by choosing paintings in an objective manner. We apply the same procedure described above to other abstract paintings, by other artists, which have a certain visual resemblance with the works of Jackson Pollock analyzed above. These works can also be broadly categorized as being abstract expressionist and were selected following similar criteria. The list of works is included on Table 2.

Fig. 6 shows a comparison of the measured Betti numbers for all Pollock's pieces and those from the other artists. In Fig. 6(a), the measured value of  $\beta_0/A$  is shown in increasing order for both Pollock and the other artists. The horizontal axis shows the painting number, according to the numbering Tables 1 and 2. In Fig. 6(b) the values of  $\beta_1/A$  are shown, corresponding to the order shown in Fig. 6(a). It is interesting to note that, when ordered in this manner, the value of  $\beta_0/A$  increases in a logarithmic manner, as depicted by the solid line in Fig. 6(a).

We can distinguish clear differences between the values of the Betti numbers for Pollock and the other artists. Interestingly, for all cases, the number of connected regions,  $\beta_0/A$ , is smaller for Pollock's works than those for the other abstract expression-

ist. Similarly, although less clear, the number of holes,  $\beta_1/A$ , is generally larger for other artists. In this sense, regardless of the degree of complexity, the works by Jackson Pollock display a notable quantifiable distinction by considering the topological invariants.

As discussed above, the degree of complexity could be determined by comparing the values of the two Betti numbers. We hypothesized that a maximum complexity was could be identified when  $\beta_0$  and  $\beta_1$  had similar values. For Pollock's case, the works dated in 1948, 1949 and 1951 had this characteristic. Therefore, to determine if Pollocks works also have a distinctive value of complexity, in comparison with other artists, we calculate the ratio  $\beta_0/\beta_1$ , for all the pieces analyzed in this study. A value of the ratio  $\beta_0/\beta_1 \approx 1$  would therefore indicate a higher level of balance and complexity. Fig. 7 shows the ratio  $\beta_0/\beta_1$  as a function of piece number for the data shown in Fig. 6. Note that, for clarity, the vertical axis is shown in a logarithmic manner. Despite the large variability of the results, it is clear that, in average, the works of Jackson Pollock are closer to  $\beta_0/\beta_1 = 1$  while for the other works  $\beta_0/\beta_1 \approx 0.68$ . Hence, again, Pollock's works have a distinct value of complexity: the pieces show a more balanced distribution of features and therefore a more refined complexity.

We have shown that a robust mathematical technique can be applied to quantify geometric complexity in abstract works. The technique, by counting connected regions and holes, clearly identifies certain features of the images. This technique measures complexity in terms of two different parameters, instead of just one like the one obtained from the fractal dimension [13–15]. We show that the complexity of the Pollock's paintings is correlated to the values of the two Betti numbers. It is interesting to note that the technique confirms that Pollock's paintings possess unique characteristics. The proposed technique could be used as tool, in addition to fractal analysis and others, for authentication. Furthermore, the

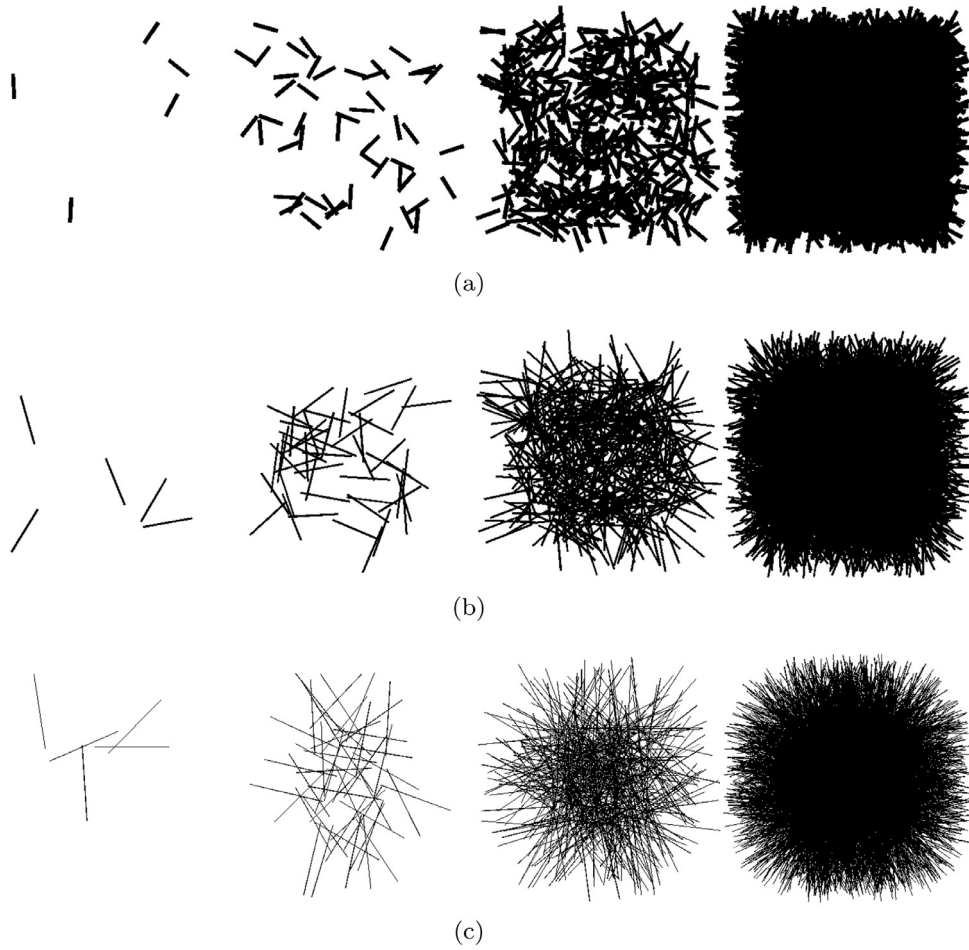


**Fig. 3.** Examples of synthetic abstract images. The size of the array is 1 by 1 (arbitrary units). Three cases are shown: short thick lines (L1W4,  $L = 0.1$ ,  $W = 4$ ); lines of medium length and thickness (L2W2,  $L = 0.2$ ,  $W = 2$ ); and long thin lines (L4W1,  $L = 0.4$ ,  $W = 1$ ). For the three images:  $N = 5$ ,  $N = 50$ ,  $N = 500$  and  $N = 5000$ , from left to right.

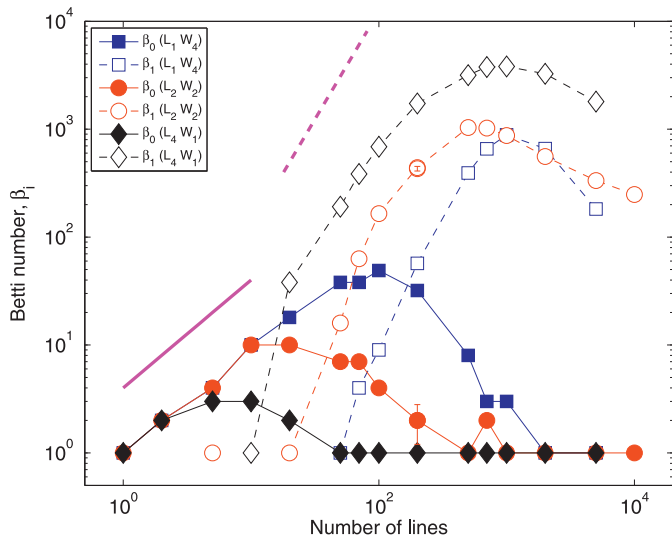


**Fig. 4.** Values of  $\beta_0$  and  $\beta_1$  as a function of number of lines for a random array for the images shown in Fig. 3. The size of the array is 1 by 1 (arbitrary units). Three cases are shown: short thick lines (L1W4, blue markers,  $L = 0.1$ ,  $W = 4$ ); lines of medium length and thickness (L2W2, red markers,  $L = 0.2$ ,  $W = 2$ ); and long thin lines (L4W1, black markers,  $L = 0.4$ ,  $W = 1$ ). The solid and dashed lines show linear and quadratic trends, respectively. (For interpretation of the references to color in this figure legend, the reader is referred to the web version of this article.)

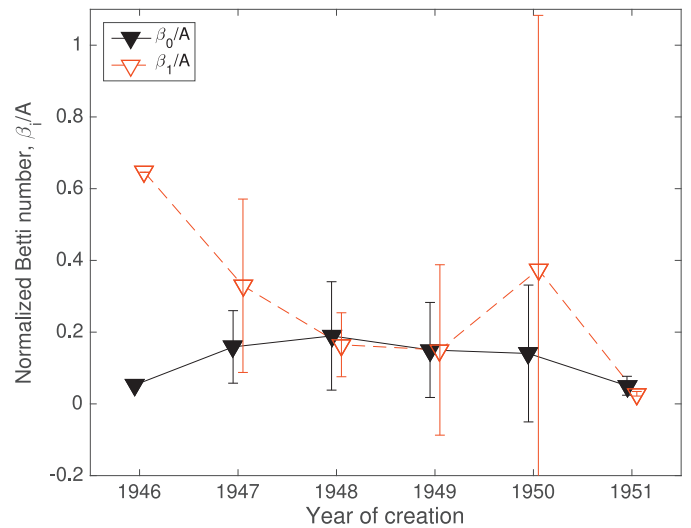


**Fig. 5.** Betti numbers per unit area as a function of time of creation. The measure of interconnected regions is characterized by  $\beta_0/A$  (black triangles); the red empty triangles show the number of holes, characterized by  $\beta_1/A$ . The data shows a slight maximum in  $\beta_0/A$  and a minimum in  $\beta_1/A$  in 1948, and a significant variability in 1950. (For interpretation of the references to color in this figure legend, the reader is referred to the web version of this article.)

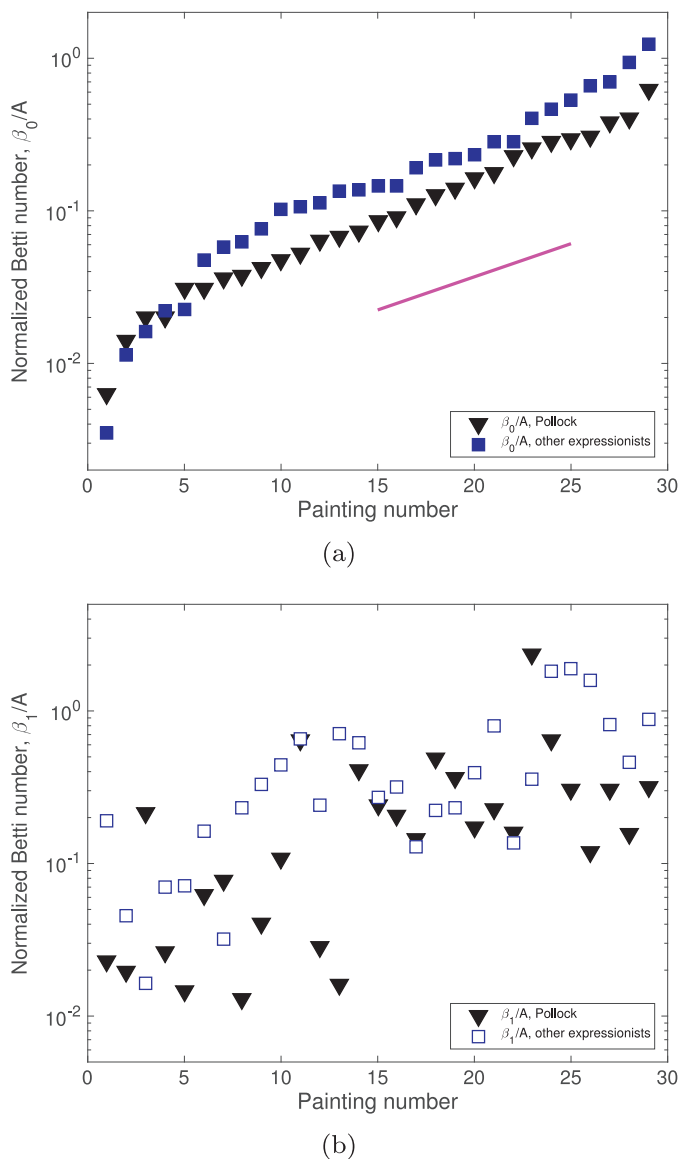


**Fig. 6.** Comparison of measured complexity: Pollock and other abstract expressionists.  $\beta_0$  and  $\beta_1$  in (a) and (b), respectively. The data is presented in increasing order considering the value of  $\beta_0$ . The line in (a) represents an exponential trend. The painting numbers can be found in Tables 1 and 2.

technique can be further improved to measure connectivity and holes at different scales or sizes of different works, to analyze the complexity of different details within a canvas or be extended to three dimensions or time variations to include other art forms and dynamic behaviors.

#### Author contributions statement

Both authors conceived the study, analysed the results, wrote and reviewed the manuscript.

#### Acknowledgments

This project was financed by PAPIIT-DGAPA-UNAM (Grant no. IN108016).

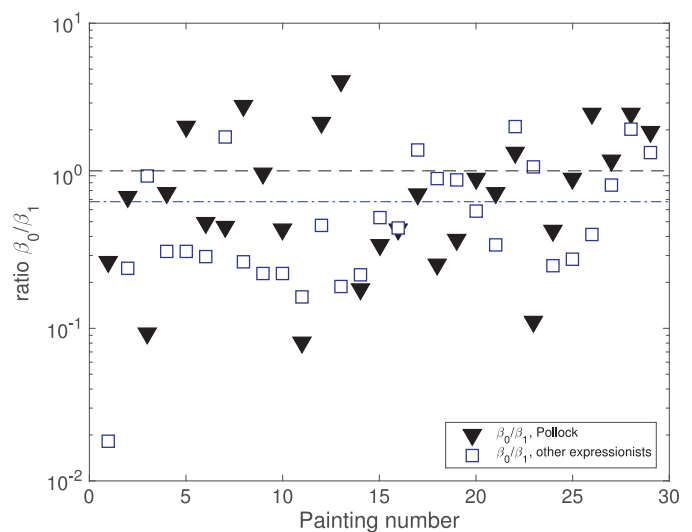


**Fig. 7.** The ratio  $\beta_0/\beta_1$  is shown as a function of painting number; the lines represent the mean values of the ratio for Pollock (black dashed line) and the other expressionists (blue dash-dotted line). (For interpretation of the references to color in this figure legend, the reader is referred to the web version of this article.)

#### References

- [1] S. Chipman, M. Mendelson, Influence of six types of visual structure on complexity judgments in children and adults, *J. Exp. Psychol. Hum.* 5 (1979) 365–378.
- [2] H.J. Eysenck, An experimental study of aesthetic preference for polygonal figures, *J. Gen. Psychol.* 79 (1968) 3–17.
- [3] A. Forsythe, M. Nadal, N. Sheehy, C.J. Cela-Conde, M. Sawey, Predicting beauty: fractal dimension and visual complexity in art, *Br. J. Psychol.* 102 (2011) 49–70.
- [4] J.L. Aragon, G.G. Naumis, M. Bai, M. Torres, P.K. Maini, Turbulent luminance in impressionist van Gogh paintings, *J. Math. Imaging Vis.* 30 (2008) 275–283.
- [5] B. Mallon, C. Redies, G. Hayn-Leichsenring, Beauty in abstract paintings: perceptual contrast and statistical properties, *Front. Hum. Neurosci.* 8 (2014) 161.
- [6] G.D. Birkhoff, *Aesthetic Measure*, Harvard University Press, Cambridge, 1933.
- [7] R. Nicki, V. Moss, Preference for non-representational art as a function of various measures of complexity, *Can. J. Psychol.* 29 (1975) 237–249.
- [8] V. Kovalevsky, Finite topology as applied to image analysis, *Comput. Vis. Graph.* 46 (1989) 141–161.
- [9] G. Burton, I.R. Moorhead, Color and spatial structure in natural scenes, *App. Opt.* 26 (1987) 157–170.
- [10] D.J. Graham, D.J. Field, Statistical regularities of art images and natural scenes: spectra, sparseness and nonlinearities, *Spat. Vis.* 21 (2007) 149–164.
- [11] S. Wolfram, *A New Kind of Science*, Wolfram Media, Champaign, 2002.
- [12] J.R. Mureika, R.P. Taylor, The abstract expressionists and les automatistes: a shared multi-fractal depth? *Sign. Proc.* 93 (2013) 573–578.
- [13] R.P. Taylor, A. Micolich, D. Jonas, Fractal analysis of Pollock's drip paintings, *Nature* 399 (1999) 422.
- [14] E. de la Calleja, F. Cervantes, J. de la Calleja, Order-fractal transitions in abstract paintings, *Ann. Phys.* 371 (2016) 313–322.
- [15] C. Redies, J. Hasenstein, J. Denzler, Fractal-like image statistics in visual art: similarity to natural scenes, *Spat. Vis.* 21 (2007) 137–148.
- [16] A. Abbot, Fractals and art: in the hands of a master, *Nature* 439 (2006) 648–650.
- [17] J. Coddington, J. Elton, D. Rockmore, Y. Wang, Multifractal analysis and authentication of Jackson Pollock paintings, in: D.G. Stork, J. Coddington (Eds.), *Proceedings of the SPIE*, 6810, 2008, pp. F1–F12.
- [18] K. Jones-Smith, H. Mathur, Fractal analysis: revisiting Pollock's drip paintings, *Nature* 444 (2006) E9–E10.
- [19] K. Jones-Smith, H. Mathur, L.M. Krauss, Drip paintings and fractal analysis, *Phys. Rev. E* 79 (2009) 046111, doi:10.1103/PhysRevE.79.046111.
- [20] J. Munkres, *Elements of Algebraic Topology*, Addison-Wesley Publishing Co., Menlo Park, CA, 1984.
- [21] L. Gottsche, The Betti numbers of the Hilbert scheme of points on a smooth projective surface, *Math. Ann.* 286 (1990) 193–208.
- [22] L. Kondic, A. Goulet, C.S. O'Hern, M. Kramar, K. Mischaikow, R.P. Behringer, Topology of force networks in compressed granular media, *Europhys. Lett.* 97 (2012) 54001–54007.
- [23] K. Xia, G. Wei, Persistent homology analysis of protein structure, flexibility and folding, *Int. J. Numer. Methods Biomed. Eng.* 30 (2014) 814–844.
- [24] C. Spänslätt, E. Ardonne, J.C. Budich, T.H. Hansson, Topological aspects of pi-phase winding junctions in superconducting wires, *J. Phys.* 27 (2005) 405701.
- [25] R. Taylor, Order in Pollock's chaos, *Sci. Am.* 287 (2002) 116–121.

- [26] J. Kosterlitz, D.J. Thouless, Ordering, metastability and phase transitions in two-dimensional systems, *J. Phys. C Solid State* 6 (1973) 1181–1203.
- [27] J.R. Mureika, Fractal dimensions in perceptual color space: a comparison study using Jackson Pollock's art, *Chaos* 15 (2005) 043702.
- [28] R.P. Taylor, A.P. Micolich, D. Jonas, The use of science to investigate Jackson Pollock's drip paintings, *J. Conscious. Stud.* 7 (2000) 137–150.
- [29] R.P. Taylor, R. Guzman, R.M. Martin, G. Hal, A.P. Micolich, D. Jonas, B. Scannell, M. Fairbanks, C. Marlow, Authenticating Pollock paintings with fractal geometry, *Pattern Recognit. Lett.* 28 (2007) 695–702.
- [30] J. Mureika, C. Dyer, G. Cupchik, Multifractal structure in nonrepresentational art, *Phys. Rev. E* 72 (2005) 046101.
- [31] C. Schneider, W. Rasband, K. Eliceiri, Nih image to ImageJ: 25 years of image analysis, *Nature Methods* 9 (2012) 671–675.
- [32] Computational homology project, <http://chomp.rutgers.edu/index.html>, 2016.
- [33] T. Kaczynski, K. Mischaikow, M. Mrozek, *Computational Homology*, Springer Verlag, New York, 2004.
- [34] L. Emmerling, Jackson Pollock, Taschen, Germany, 2003.